A COMPUTATIONAL STUDY OF THE AERODYNAMICS OF A SPINNING CYLINDER IN A CROSSFLOW OF HIGH REYNOLDS NUMBER

E. R. Gowree and S. A. Prince
Centre of Aeronautics, City University London
erwin.gowree.1@city.ac.uk; s.a.prince@city.ac.uk

Abstract

A Computational Fluid Dynamics (CFD) analysis of the high Reynolds number (Re ≈ 94k) flow around a quasi-2D spinning cylinder in a crossflow, using a high resolution 3D time marching unsteady Navier-Stokes solver was conducted. The lift coefficients predicted were in fair agreement with experimental results except in the Inverse Magnus Effect region (0.4 < Ω < 0.7). The fact that these simulations were computed as purely laminar boundary layer flows, and failed to resolve any evidence of the Inverse Magnus Effect, would tend to support the proposition that the Inverse Magnus Effect is associated with boundary layer transition. The trends in the experimentally measured shedding frequency with cylinder spinning speed were captured reasonably well by the numerical model which resolved the initial rise in vortex shedding frequency with increased Ω, followed by a rapid fall. At Ω ≈ 2, suppression in the vortex shedding was observed and this finding demonstrates that vortex shedding degradation and suppression with increase in velocity ratio is still present even for high Re flow in the subcritical regime.

1 Introduction

An attempt to harness the energy generated from the 'Magnus Effect' from spinning cylinders was made by Anton Flettner [1] in the mid 1920's. Later he demonstrated the concept by replacing the conventional sails by spinning circular cylinders for the propulsion of large ships, through the modification of the 'Buckau' and 'Barbara'. However, being a function of the ambient wind speed the cylinder's performance was vulnerable, and due to the large availability and low cost of fuel in that era the idea was rendered redundant.

The UAV (unmanned aerial vehicle) or MAV (micro air vehicle) industry is currently expanding due to these crafts ability to operate in hostile and inhospitable environments. An elaborate feasibility study conducted by C. Badalamenti [2] during his Doctoral research has demonstrated that spinning cylinders can be an alternative for conventional fixed wings when high lift to drag ratio is required. In addition, unlike conventional wings spinning cylinders are not constrained by stall and therefore could therefore offer increased payload capability. Further benefits in mission performance might be achieved during operations in high density ambient conditions such as in Polar latitudes. One interesting application where high lifting capability would be essential, and which needs some investigation, would be for flight vehicles for the unmanned exploration of extra-terrestrial environments such as the surfaces of Mars or Titan.

The lack of application for rotating cylinder wings due to practicality issues at high subcritical Reynolds number (*Re*) has hampered the research directed towards understanding the highly complex flow physics, especially within the viscous layer and the behaviour of the vortical wake. Experimental investigations at high *Re* are usually hindered by structural dynamics issues related to the model and there are still arguments on the vortex shedding mechanism at high velocity ratios. Therefore, a numerical study has been launched to investigate whether the vortex shedding and the aerodynamics forces can be captured qualitatively at high *Re* and spinning speed using CFD, bearing in mind that the 'Inverse Magnus Effect' might present a challenge due to the transitional nature of the boundary layer.

1.1 The Magnus Effect

The result of the survey on Magnus Effect conducted by Swanson [3] in the early 1960's has demonstrated that in the grand scheme of things the magnitude of the lift coefficient (C_L) generated by a spinning cylinder increases with increase in the ratio of peripheral to freestream velocity ratio (Ω). The prime observation suggested that C_L was a function of the aspect ratio (*AR*), end effects and Reynolds number and the maximum lift coefficient (C_{Lmax}) of 4π, which Ludwig Prandtl initially suggested can be exceeded by use of cylinders with large *AR*. According to Swanson [4] and Krahn [5] the initial increase in C_L with increase in Ω was due to the asymmetrical laminar boundary layer separation between the upper and the lower surface. A larger extent of attached boundary layer and the associated region of suction, on the upper surface, compared with the lower surface, results in increased lift.

Swanson suggested that this shift in the separation point was a consequence of the displacement of the boundary layer origin which progressed along the direction of rotation as shown in figure 1.

The most recent experimental study to prove the dependency of C_L on *AR* was undertaken by Badalamenti and Prince [6] in 2008 on a cylinder with $AR = 5.1$. A comparison of the authors' results with previous experimental results for a range of *AR* is shown in Figure 2 (more information of the references quoted in the legend can be obtained from reference 4). It was shown that an increase in *AR* would lead to a higher achievable maximum lift, and for low and medium *AR* ($1.5 < AR < 6$) the point where C_L starts to plateau (maximum point followed by a constant lift) could be shifted upward through the introduction of endplates which were at least 1.5 times the diameter of the cylinder.

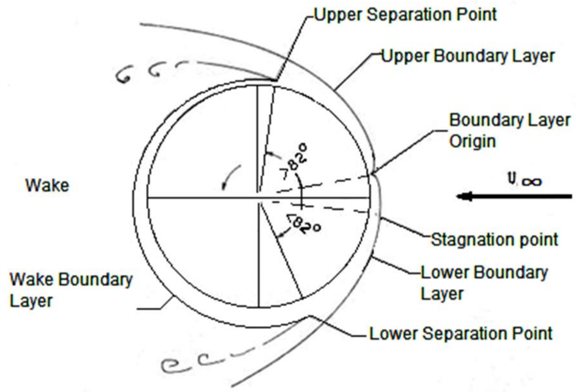

Fig 1: Schematic reprensentation of the viscous flow engulfing a spinning cylinder. [3]

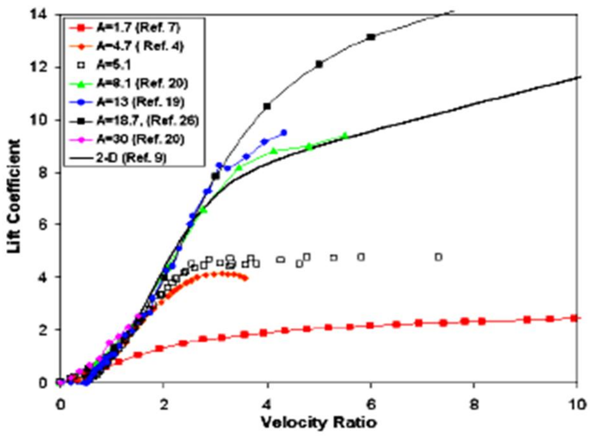

Fig 2: The effect of AR on the amount of lift generated. [2]

1.2 The Inverse Magnus Effect

Based on Swanson's analysis, unlike the *AR*, increasing the *Re* of the flow has a more complicated effect on the magnitude of the aerodynamic forces, especially at $\Omega < 1.0$. From Swanson's experimental results shown in Figures 3(a) and 3(b) (where the *Re* of each corresponding cases has been quoted in Table 1). For $Re \geq 61k$[1] a loss in C_L similar to the post stall characteristic on an aerofoil can be observed, this effect has been referred as the 'Inverse Magnus Effect' which was initially presented by Lafay [7] in 1910. The effect became more pronounced for $225k \leq Re \leq 365k$ as there was rather an initial decrease in C_L. A similar trend was encountered by Badalamenti et al. at $Re > 43k$, therefore it might be fair to hypothesise that this effect is dependent on the

[1] 'k' represents 10^3

interaction of the fluid and the amplification of the disturbances within the viscous layer.

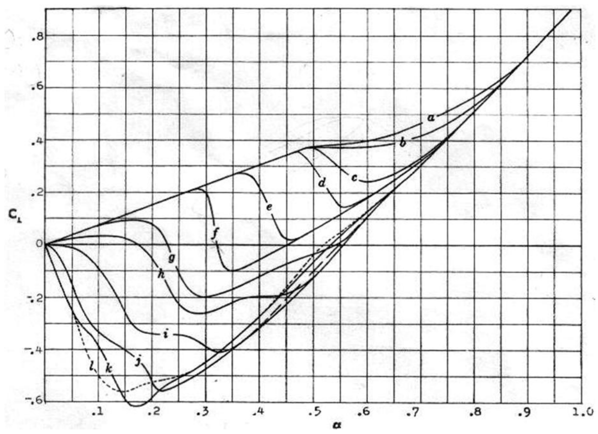

Fig 3(a): The effect of Re on the variation of C_L with Ω [3].

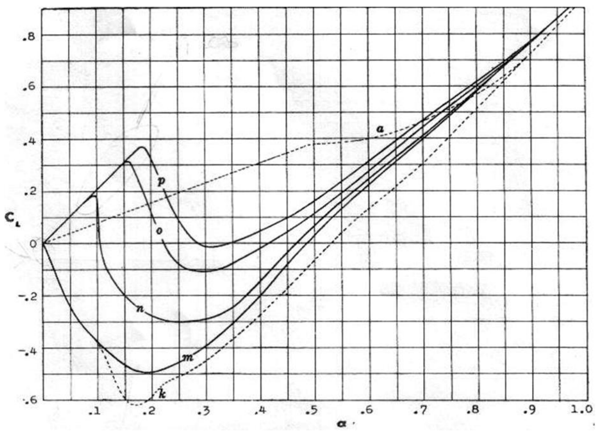

Fig 3(b): The effect of Re on the variation of C_L with Ω [3].

Prior to the detailed analysis of the Inverse Magnus Effect, which was observed at $\Omega > 0.35$ in the case considered above, it might be helpful to investigate the nature of the viscous layer in that flow regime. Referring to figure 3, which was produced by Zdravkovich [8] for the *Re* of the current investigation, on a stationary cylinder the flow is essentially subcritical and in the upper limit of transition in the shear layer regime. This fact can also be supported by the drag measurement performed by Swanson (see 'Figure 6' of reference 3) on the stationary cylinder where a sudden decrease in C_D with further increase in *Re* was observed for $Re > 99k$ (case 'e'). This behaviour is common with low speed flows around bluff bodies, and is a direct effect of the reduction in the size of the wake due to the transitional nature of the boundary layer which stays attached over a further extent once in their turbulent state.

In this regime the viscous layer appears to be very vulnerable to small instabilities in the flow. Keeping this in mind, Swanson suggested that as Ω is increased the 'relative Reynolds number', $Re_{rel} = Re(1 \pm \Omega)$, of the boundary layer on the lower surface would increase with respect to the freestream *Re* due to an increase in relative velocity, and vice versa, and thus it would transition to turbulent. In this state it would stay attached further downstream and the suction on the surface concerned would be extended, hence reducing the net lift generated. This effect would become more pronounced with an increase in Ω until both of the boundary layers become fully turbulent, which will be marked by the minimum point in the trend.

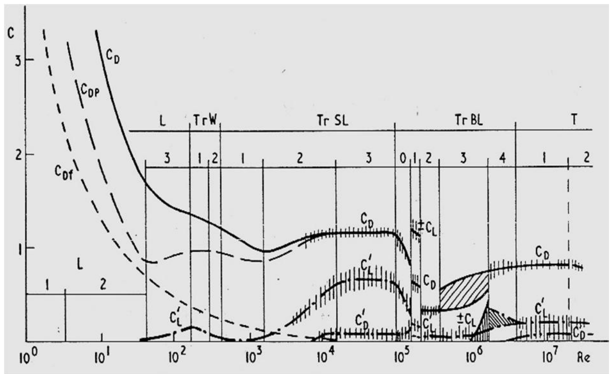

Fig. 4: The effect of Re on the magnitude of aerodynamic forces generated by a stationary circular cylinder in a crossflow [8].

Table 1: The Re for the corresponding cases represented in Figure 3(a) and 3(b).

Case	Re	Case	Re
a	36k	*i*	225k
b	49k	*j*	260k
c	61k	*k*	295k
d	79k	*l*	325k
e	99k	*m*	365k
f	128k	*n*	420k
g	152k	*o*	450k
h	182k	*p*	501k

1.3 Vortex Shedding

Stationary circular cylinders in crossflow are known to undergo periodic vortex shedding (Von Karman Vortex Street). The vortex shedding can commence at *Re* as low as 65 where the flow is purely laminar and is still present in fully developed turbulent flow *of Re* $= 8x10^6$ [8]. Experimental work conducted by Jaminet et al. [9] has demonstrated that the vortex shedding can be initiated at $Re < 48$ if a steady rotation is introduced. However, the most interesting observation was the fact that at a certain rotational speed the vortex shedding was completely suppressed. According to Badalamenti and Prince [10] for the *Re* regime where periodical vortex shedding is present there is a common accord in the literature to confirm the existence of a critical rotational velocity, Ω_c at which suppression of shedding will occur. The latter suggested that Ω_c increases with increasing *Re* and is invariable at $\Omega_c \approx 2$ for $Re \geq 200$, except during the investigation conducted by Chew et al. [11], where $\Omega_c \approx 3$ was achieved.

From Badalementi and Prince, [10] the computational study at low *Re* undertaken by Stojkovic et al [12], [13] and Mittal et al. [14] suggested that there might be a recurrence of a secondary mode of vortex shedding. This effect was presumed to occur in a very confine range of high Ω with strong dependency on the *Re*. It was speculated by Stojkovic et al [13] that the effect is likely to be present at higher *Re* even if their analysis was conducted at $Re \leq 200$. Paradoxically in the higher *Re* experimental analysis of Massons et al. [15] at $Re = 2k$, Diaz et al. [16],[17] at $Re = 9k$ and Tanaka et al. [18] at $45k \leq Re \leq 214K$ for a velocity ratio of $\Omega \leq 4$, $\Omega \leq 2.5$ and $\Omega \leq 1$ respectively, there were no features representing the secondary mode of shedding. Badalamenti et al. suggested that the absence of the secondary mode in these cases might be attributable to the low velocity ratios.

Nevertheless, the experiments of Badalamenti et al. [6], performed at $41k \leq Re \leq 98k$ and $\Omega \leq 4$, vortex shedding suppression was observed at $\Omega \approx 2$ and at $\Omega \approx 3$ shedding resumed at $Re = 41k$. The latter suggested that the existence of the secondary mode might be strongly related to the *AR*, where low *AR* causes the trailing vortices to migrate inboard and the use of cylinders with larger *AR*, such as in the experiments mentioned above, might be another reason why the secondary shedding mode did not appear. However there was no mention of the occurrence of the secondary mode at $Re = 98k$. This might be due to the inability to acquire meaningful data due to the hindrance caused by structural dynamics limitation of the experimental model at high *Re*.

2 Procedures for Numerical Analysis

The circular cylinder model for the current investigation was the one used during the Badalamenti et al. study, with a diameter of 89 mm and $AR = 5.1$. The freestream *Re* based on the cylinder diameter was kept constant at 94k and following the initial case where the cylinder was kept stationary, further computational analysis was conducted by rotating the cylinder for $\Omega \leq 4$.

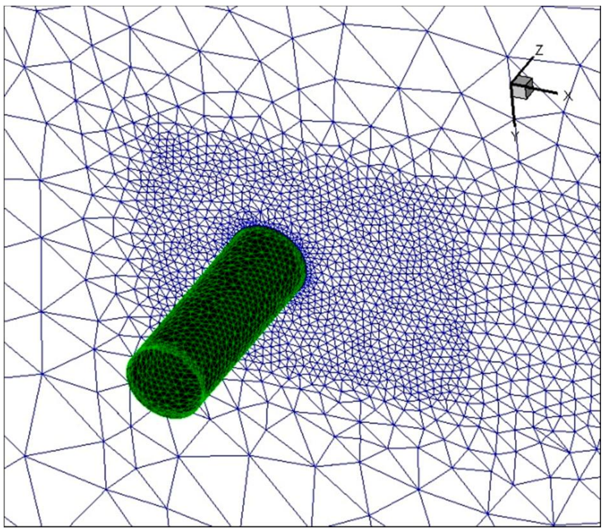

Fig 5: Computational surface grid (green) and the left hand periodic plane (blue) for the course grid.

Table 2: The numbers of cells each mesh type contains

Grid Type	Number of cells
Fine	1,200,000
Medium	605,800
Coarse	323,700

Using a commercial solver, the Navier Stokes equations were solved through an explicit time marching, finite volume scheme, with nominally 2nd order accuracy in both space and time assuming a purely laminar flow. Time steps of 0.00025 seconds were employed, with convergence defined at five orders of residual convergence or 10,000 iterations. Initially, the simulations were performed on 3D hybrid grid (unstructured outer grid with embedded structured boundary layer zone) of 1.2 million cells, which modelled the quasi-3D flow over a 3D spanwise section (centre section of the experimental model cylinder) using periodic boundary conditions to model a quasi-infinite spanwise length cylinder. A grid sensitivity for the non-spinning case was performed with grid sizes as given in table 2. The course grid is shown in figure 5. The first cell height adjacent to the cylinder surface was set at $1x10^{-5}$D for all grids, giving about 20 cells in the attached laminar boundary layers for the medium grid case.

The flow field contours were analysed using Tecplot360. SPIKE, was used to compute the Fast Fourier Transform (FFT) of a large enough sample of computed lift and drag signals in order to analyse the frequency of vortex shedding, for an FFT size of 2048, using the Hanning window.

3 Results and discussion

The current numerical result was compared with experimental results of Badalamenti et al. [2], [6]. For the non rotating cylinder case, the force results for using the fine grid corresponded well with those obtained with the medium grid. Also, at low velocity ratio the trend in the lift computed using the medium grid was in fair agreement with the experimentally measured lift, as opposed to the Coarse grid and therefore the rest of the simulation was conducted on the Medium grid.

While the ‘Inverse Magnus Effect’ is an important topic of this paper, the main aim of the current analysis was to check whether a qualitative understanding of the general trend in lift and drag and vortex shedding suppression could be obtained from a RANS calculation at relatively large *Re*.

3.1 The Aerodynamic Forces

The highly unsteady nature of the flow past a spinning cylinder has been demonstrated in figure 6, which shows the periodic variation of lift coefficient for a time period of 2 seconds for the case of $\Omega = 0.5$, 0.7 and 1.0. The arithmetic mean of the sample of unsteady C_L and C_D was estimated for each velocity ratio and this was compared with the experimental result obtained by Badalamenti et al. [2] at *Re 94k*. At low velocity ratios, $\Omega \leq 0.5$ the initial increase in C_L estimated numerically seems to be in good agreement with the experimentally measured cases, as shown in figure 7. This shows that the ‘Magnus Effect’ has been successfully captured by the CFD method. As mentioned in the introduction section, for these Ω the boundary layer is purely laminar and bound to undergo transition in the shear layers.

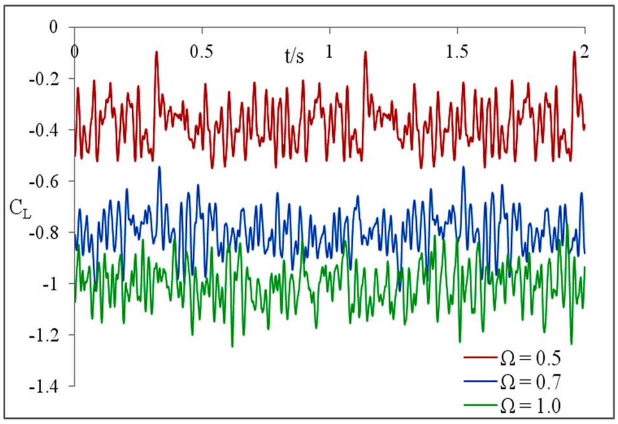

Fig. 6: The variation of numerically estimated lift with time.

However, for $\Omega > 0.5$, the numerical method seemed to be performing poorly as the ‘Inverse Magnus Effect’ was not captured at all, and for $\Omega > 1$ the overall magnitude of the C_L was under-predicted. At high subcritical *Re* according to Swanson [3] and Badalamenti et al. [6] the ‘Inverse Magnus Effect’ region is a result of transition occurring within the boundary layer. Swanson suggested that the side travelling in the opposite direction of the freestream velocity, transitions to turbulent and stays attached to a larger portion of the cylinder's surface, thus, increasing the suction on that side, resulting in a decrease in the net lift.

The crucial point to be noted here is that the current numerical study was conducted assuming a purely laminar boundary layer and RANS modelling was used to capture the macro-structures inside the turbulent wake assuming transition will occur in the shear layers for all velocity ratios. Therefore, the inability to predict the C_L accurately in the 'Inverse Magnus Effect' region using the chosen numerical scheme supports the argument that this effect arises mainly due to the transitional nature of the boundary layer. The numerical method was clearly unable to capture the amplification of initial disturbances leading to transition, which always poses a challenge for RANS modelling.

While the authors agree with Swanson regarding the theory that the Inverse Magnus Effect is related to transition in the boundary layer, the model to help explain this involving the 'relative Reynolds number' is suggested to be somewhat questionable from a purely physical point of view. This is because at $\Omega \geq 1$, the Re_{rel} on the upper surface will be equal to zero or negative, which is a confusing concept.

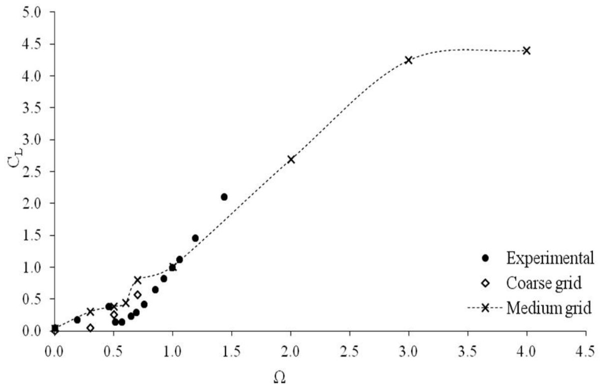

Fig. 7: Comparison of computational C_L obtained using both the medium and coarse grid with experimental result of Badalamenti et al [2].

The authors suggest a different approach to explain qualitatively the transition process within the viscous layer, by isolating the adjacent viscous layer (friction) created by the rotation of the cylinder and the effect of the freestream flow. Effectively, the freestream velocity will act in favour of the boundary layer on the surface travelling in the same direction of the freestream fluid, by providing extra momentum through the process of entrainment. On the side travelling in the opposite direction of the freestream flow, however, energy will be dissipated from the boundary layer, therefore increasing its susceptibility to disturbances. This effect will amplify the instability of the boundary layer which favours the asymptotic nature of the velocity profile, hence leading to a turbulent reattachment.

From figure 8 the numerically estimated C_D using both Medium and Coarse grids show poor correlation with experimentally measured drag, where surprisingly the Coarse grid appears to be performing better. Unlike the experimental result there was no initial rise in C_D for $\Omega \leq 0.5$ and the absolute drag level as well was under-predicted. Nevertheless, looking at the trend in the reduction in C_D with increase in Ω, which was associated with the reduction in the width of the wake due reattachment of the turbulent boundary layer, is successfully captured. The numerical method seems to be able to handle the large scale turbulence in the wake and hence capture qualitatively the reduction of form drag.

It is very important to note, at this stage that, since the current simulations employed a periodic boundary condition to enforce an infinite span model while still capturing quasi-3D flow structure. The present CFD results will therefore not capture any drag component associated with the effects of the cylinder ends, which would appear in the results of Badalamenti et al., whose model *AR* was 5.1. For this reason a direct comparison of the magnitude of the drag prediction was always expected to show a significant underprediction. This is certainly evident in figure 8. No attempt has been made here, to assess the effect of the model ends.

A sudden rise in drag was observed in the experimental result once the Ω passed the Inverse Magnus Effect (Ω > 1) phase and this was mainly due to increase in lift which triggers the induced drag, whereas in the current case only a slight rise in drag was observed at Ω ≥ 1.

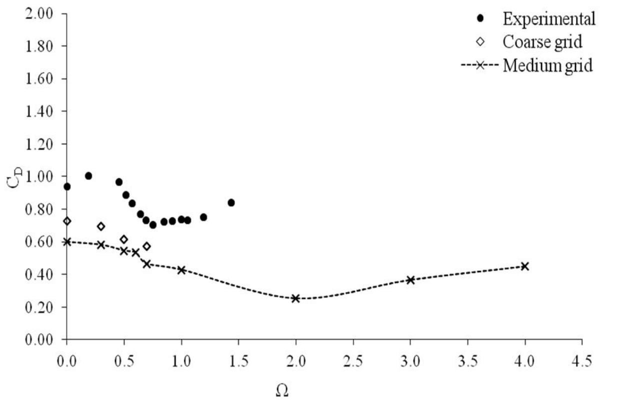

Fig. 8: Comparison of computational C_D obtained using both the medium and coarse grid with experimental result of Badalamenti and Prince [2].

3.2 Vortex Shedding

The highly periodic nature of the C_L shown in figure 6 confirms the fact that, similar to stationary cylinders, spinning cylinders also tend to shed vortices in a cyclic nature. For the sample of fluctuating C_L data, a Fast Fourier Transform was conducted using the Hanning windowing function for a block size of 2048 and the result was expressed by Power Spectra, a sample of which are shown in figure 9. From the 4 PSDs, very large initial amplitude was observed for the entire velocity ratio range, which is common to these kinds of unsteady flows, but is not associated with vortex shedding. Therefore, the secondary peak was used to quantify the frequency of vortex shedding and this frequency was used to estimate the shedding Strouhal number (*St*) at each velocity ratio, which was compared with the experimental estimation of Badalamenti and Prince [10], Tanaka and Nagano [18] and Diaz et al. [16], [17].

For the stationary case the current numerically estimated *St* seems to be in fair agreement with the value estimated by Badalamenti and Prince and Tanaka and Nagano. At low velocity ratios, $\Omega < 1$, a small level of scatter was found in the results, but the trend was captured well. The Badalamenti and Prince results, for $\Omega \leq 1$, show a rise in *St* with Ω, whereas, in the case of the rest of the authors this change was very small, if not constant. According to Badalamenti this was due to the existence of the 'lock on' phenomena which was caused by vibration of the cylinder. For $\Omega = 1$ the numerically estimated value of *St* was in good agreement with both Badalamenti and Prince and Diaz et al.

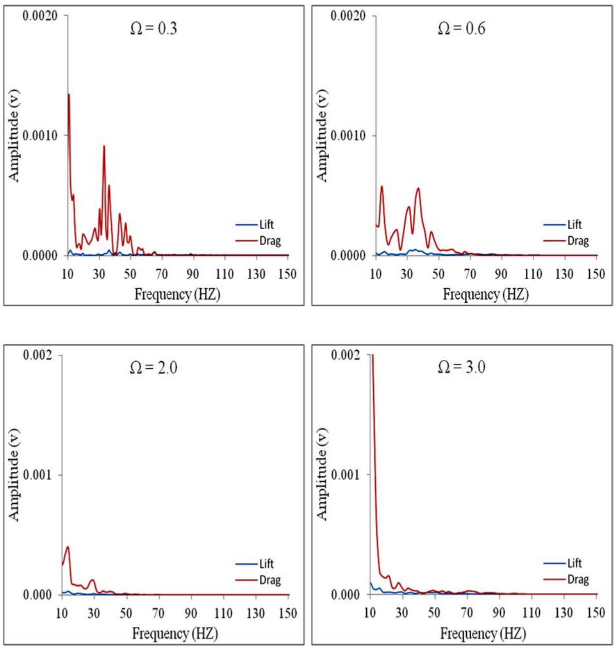

Fig. 9: PSD of the periodic lift and drag captured during the computation.

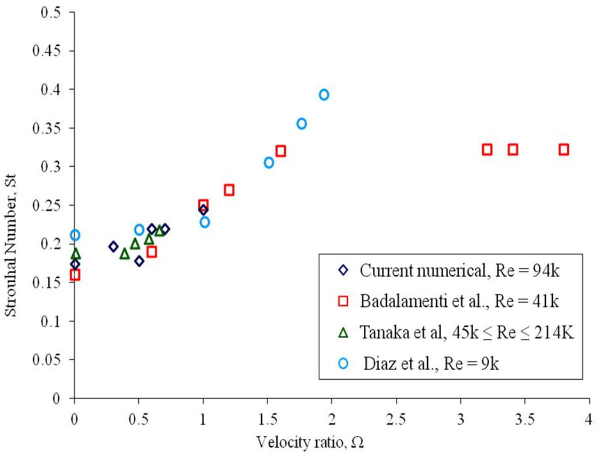

Fig. 10: Variation of Strouhal Number with velocity ratio based on the shedding frequency and a comparison with experimental data of Badalamenti and Prince. [10], Tanaka and Nagano [18] and Diaz et al. [16], [17].

3.3 Suppression of Vortex Shedding

As mentioned in the literature review, the introduction of rotation acts to promote the degradation of vortex shedding and in most of the cases studied at $\Omega \approx 2$ the vortical structures had disappeared except in the case of Chew at al. [11] where it occurred at $\Omega \approx 3$. From the data of figure 9, if the initial peaks were neglected, the reduction in the amplitude of the second peak shows the loss in the energy of the signal, hence a reduction in vorticity. At $\Omega = 2$ the amplitude of the peak is very low and at $\Omega = 3$ there was the total absence of any periodicity. This result seems to be in good agreement with the experimental prediction of Badalamenti and Prince [10] where shedding suppression was noticed at $\Omega \approx 2$. Figure 11 shows the contours of total pressure in the centreplane of the cylinder, a reduction of the low pressure region inside the wake can be observed with increasing Ω. Therefore this provides an additional qualitative confirmation of the suppression of vortex shedding.

Unlike the results from Badalamenti and Prince there was no indication of the development of the secondary mode of vortex shedding, even at $\Omega = 4$ (power spectra or contour plot not shown here). From the literature review conducted by Badalamenti and Prince it was suggested that this effect occurs only in a confine envelope of Ω, and with increase in *Re* it appears earlier. Given the crudeness of the numerical scheme the results at high Ω might be highly questionable due to the fully developed turbulent nature of the flow. In addition Badalamenti and Prince suggested that during their experiment the secondary shedding mode was strongly related to the *AR*, whereby for small *AR* the trailing vortices tend to migrate inboard. The inability to capture the 3D effects accurately due to the periodic boundary condition to replicate a quasi 3D behaviour might also explain why the resumption of shedding, as the secondary mode, was not captured by the numerical scheme.

It has been demonstrated above that the numerical scheme struggled to handle the flow during the transitional regime when the Inverse Magnus Effect was encountered. However, the sensible trend in *St* and the ability to capture qualitatively the degradation of vortex shedding and the trend in the decrease in form drag by the numerical scheme supports the view that the large structures are being successfully captured inside the wake. Based on this argument it is very questionable whether there is the existence of the secondary vortex shedding mode for this high subcritical *Re*. Thus further simulation will be required using a higher fidelity numerical scheme for higher velocity ratio and better end boundary condition to capture the 3D nature of the flow more accurately, should direct comparison with experimental data is required.

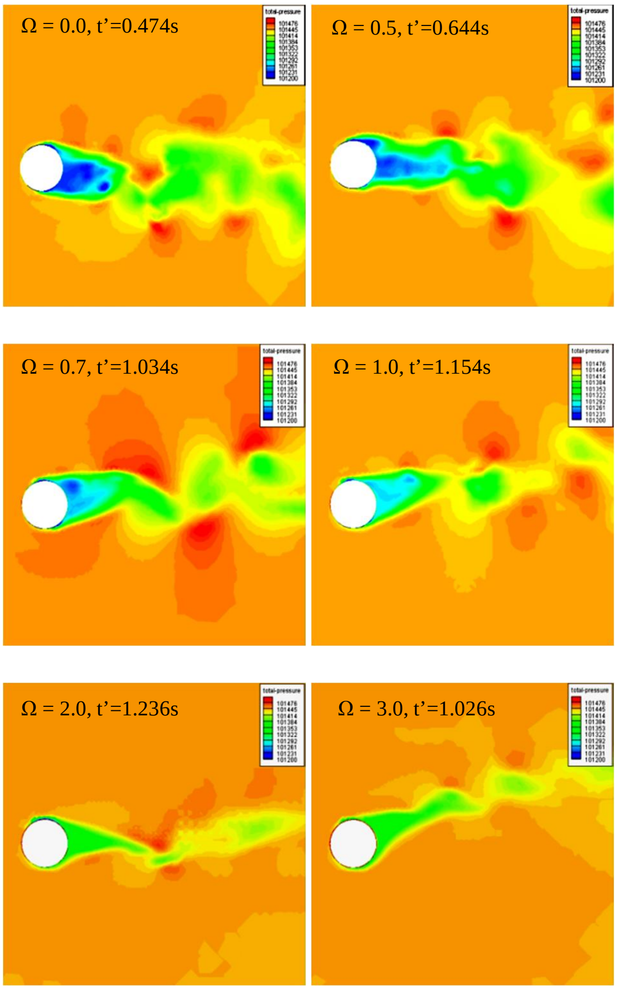

Fig. 11: Computed total pressure contours on the centreplane – illustrating the effect of rotation speed on vortex shedding suppression.

4 Conclusions

The conclusions derived from this study are:

- Solution of the time-accurate Reynolds Averaged Navier-Stokes equations is able to capture the large scale vortical unsteady flow shed from a static and a rotating circular cylinder in subcritical (fully laminar boundary layers) crossflow. Such a methodology is able to successfully resolve the overall trends in lift and drag force, and shedding frequency behaviour with rotational speed.

- For crossflows in the critical Reynolds number range, as investigated in this study, solution of the laminar RANS equations has been shown to be inadequate to resolve the "Inverse Magnus Effect" observed in many experimental investigations. This finding supports the view that this effect is associated with the early transition, on the lower side of the rotating cylinder where its surface moves against the freestream. This physical process cannot be described in the laminar CFD model used in this study.

The authors intend to undertake further numerical study of the Inverse Magnus Effect by employing much finer computational grids, obtaining more data in the region $0.3 < \Omega < 0.8$ and investigating the effect of simulating (forcing) the transition to turbulence of the lower surface boundary layer, while maintaining the upper surface as laminar. The results of these studies may shed further light on the physical origin of the Inverse Magnus Effect.

References

[1] Flettner, A. "The *Flettner Rotorship*" Journal of Engineering, Vol. 19, pp117-120, 1925

[2] Badalamenti, C. "*On The Application of Rotating Cylinders to Micro Air Vehicles*". PhD. Thesis, City University London, 2010.

[3] Swanson, W. M., "*The Magnus Effect: A Summary of Investigation to Date*", *ASME Transactions Series D, Journal of Basic Engineering.* Vol. 83. pp. 461-470. 1961

[4] Swanson, W. M,. "*An Experimental Investigation of the Magnus Effect*", Case Institute of Technology , 1956. OOR Proj. No. 1082.

[5] Krahn, E. "*The Laminar Boundary Layer on a Rotating Cylinder in Crossflow*", NAVORD Rep. 4022 , Aerobal. Res Rep. 288 , 1955.

[6] Badalamenti, C. and Prince, S. "*The Effects of Endplates on a Rotating Cylinder in Crossflow*" AIAA Paper 2008-7063. AIAA Applied Aerodynamics Conference, Hawaii, Aug. 2008.

[7] Lafay, M. "*Sur L'Inversion du Phenomene de Magnus.*" Comptes-Rendus, Vol. 151. 1910.

[8] Zdravkovich, M., "*Flow around Circular Cylinders. Vol. 2 : Applications*" Oxford University Press Inc., New York, 2003.

[9] Jaminet, J. F., J F and Van Atta, C. W. "*Experiments on vortex shedding from rotating circular cylinders*", AIAA Journal, Vol. 7, No. 9, pp1817-1819, 1969

[10] Badalamenti, C. and Prince, S. "*Vortex shedding from a rotating circular cylinder at moderate sub-critical Reynolds numbers adn high velocity ratio*" Paper 2008-3.10.5 26th Intenational Congress of the Aeronautical Sciences, 2008.

[11] Chew, Y. T., Cheng, M. and Luo, S. C., "*A numerical study of flow past a rotating circular cylinder using a hybrid vortex scheme*", Journal of Fluid Mechanics, Vol. 299, pp35-71, 1995.

[12] Stojković, D., Breuer, M. And Durst, F., "*Effect of high rotation rates of laminar flow around a circular cylinder*", Physics of Fluids, Vol. 14, No. 9, pp3160-3178, 2002.

[13] Stojković, D., Schön, P., Breuer, M., and Durst, F., "*On the new vortex shedding mode past a rotating circular cylinder*", Physics of Fluids, Vol. 15, No. 5, pp1257-1260, 2003.

[14] Mittal, S., and Kumar, B., "*Flow past a rotating cylinder*", Journal of Fluid Mechanics, Vol. 476, pp303-334, 2003.

[15] Massons, J., Ruiz, X. and Diaz, F. "*Image Processing of Near Wakes of Stationary and Rotating Cylinders*", Journal of Fluid Mechanics, Vol.204, pp 167-184, 1989

[16] Díaz, F., Gavaldà, J., Kawall, J. G., Keffer, J. F. And Giralt, F. "*Vortex shedding from*

a spinning cylinder", Physics of Fluids, Vol. 26, No. 12., pp3454-3460, 1983.
[17] Díaz, F., Gavaldà, J., Kawall, J. G., Keffer, J. F. And Giralt, F. "*Asymmetrical wake generated by a spinning cylinder*". AIAA Journal, Vol. 23, No. 1, pp49-54, 1985.
[18] Tanaka, H. and Nagano, S. "*Study of the flow around a rotating circular cylinder*" Bulletins of the Japanese Society of Mechanical Engineers, Vol. 16, No. 92, pp234-243, 1973.

Copyright Statement